A parameterization of flow separation over subaqueous dunes

Andries J. Paarlberg, C. Marjolein Dohmen-Janssen and Suzanne J.M.H. Hulscher

Department of Water Engineering and Management, University of Twente, Enschede, The Netherlands.

Paul Termes

HKV Consultants, Lelystad, The Netherlands

Andries. J. Paarlberg, Department of Water Engineering and Management, University of Twente, Horst Building, P.O. Box 217, 7500 AE, Enschede, The Netherlands. (a.j.paarlberg@ctw.utwente.nl)

Abstract. Flow separation plays a key role in the development of dunes, and modelling the complicated flow behaviour inside the flow separation zone requires much computational effort. In order to make a first step towards modelling dune development at reasonable temporal and spatial scales, a parameterization of the shape of the flow separation zone over two-dimensional dunes is proposed herein, in order to avoid modelling the complex flow inside the flow separation zone. Flow separation behind dunes, with an angle-of-repose slip face, is characterized by a large circulating leeside eddy, where a separation streamline forms the upper boundary of the recirculating eddy. Experimental data of turbulent flow over 2D subaqueous bedforms are used to parameterize this separation streamline. The bedforms have various heights and height to length ratios, and a wide range of flow conditions is analyzed. This paper shows that the shape of the flow separation zone can be approximated by a third-order polynomial as a function of the distance away from the flow separation point. The coefficients of the polynomial can be estimated, independent of flow conditions, based on bedform shape at the flow separation point and a constant angle of the separation streamline at the flow reattachment point.

1. Introduction

Flow over sandy river beds often leads to the formation of a regular bed morphology such as dunes [e.g., *Allen*, 1968; *Best*, 2005]. Because of flow separation and associated energy dissipation, dunes significantly influence flow resistance [e.g., *Vanoni and Hwang*, 1967; *Wijbenga*, 1990; *Ogink*, 1989; *Julien et al.*, 2002]. For many water management purposes it is of great importance to enable prediction of dune dimensions and the resulting flow resistance, especially during floods.

To simulate turbulent flow over dunes numerically, the bed is often assumed rigid and non-erodible. However, increasing computational power has recently led to the development of morphodynamic models treating the flow, bed morphology and sediment transport in a coupled manner. *Tjerry and Fredsøe* [2005] calculate dune dimensions and shapes of solitary dunes, by relating sediment transport to the time-averaged bed shear stress. *Nelson et al.* [2005] have shown that a large eddy simulation model with non-hydrostatic pressure and a rigid lid water surface boundary, in combination with a sediment transport model taking turbulent fluctuations of the bed shear stress into account, realistically models dune development. In continuation of this work, *Giri and Shimizu* [2006] improved the model of *Nelson et al.* [2005] by using flow equations with the unsteady term retained and a free water surface condition. Although model results are promising, a disadvantage of these numerical models is their complexity regarding solving the flow field, especially when the flow has to be calculated repeatedly for each bed morphology update. Furthermore, it is yet unfeasible to yield simulations with floodwaves and long domains.

In their morphodynamic model, *Jerolmack and Mohrig* [2005] excluded the necessity of computing the flow field by assuming a nonlinear relationship between the local bed shear stress and bed topography. To reduce the required computational effort, *Onda and Hosoda* [2004] used a depth-averaged hydrostatic flow model, including vertical acceleration terms, to simulate dune development. Although *Jerolmack and Mohrig* [2005] and *Onda and Hosoda* [2004] were able to simulate dune morphology over long domains, flow separation and its effects on the flow field and sediment transport were not included in their simulation models. However, there are several indications that flow separation, and associated turbulence and shear layer formation, are important for dune morphodynamics [e.g., *Nelson et al.*, 1995; *Bennett and Best*, 1995; *Walker and Nickling*, 2002; *Sumer et al.*, 2003].

Hulscher and Dohmen-Janssen [2005] argued that offshore sand waves and river dunes are similar features, with respect to their dimensions and processes responsible for their formation. *Paarlberg et al.* [2005] applied a model, originally developed to predict the dimensions of offshore sand waves [see *Van den Berg and Van Damme*, 2005], to river conditions. The flow model is based on the 2-dimensional vertical (2DV) hydrostatic shallow water equations with a constant eddy viscosity over the flow depth, and with bed load sediment transport included using a Meyer-Peter-Müller type of equation. It was shown that in cases without flow separation, dune development could be reproduced qualitatively. However, because of the hydrostatic pressure assumption, flow separation could not be captured by the model. To enable simulation of dune development from an initial disturbance to fully grown equilibrium dunes, flow separation therefore needs to be taken into account in any morphodynamic model.

To predict the evolution of solitary aeolian desert dunes, *Kroy et al.* [2002] included a parameterization of flow separation in their morphodynamic model. *Kroy et al.* [2002] parameterized the shape of the separation streamline, which forms the upper boundary of the flow separation zone, on the basis of numerical computations of air flow over bedforms. The flow was computed using the separation streamline as an artificial 'bed' in the region of flow separation, effectively avoiding the necessity of modelling the complicated flow behaviour inside the flow separation zone.

To keep computational effort to a minimum, but retain the process of flow separation in a simple manner in the morphodynamic model of *Paarlberg et al.* [2005], a similar approach to that adopted by *Kroy et al.* [2002] can be used. The present paper will analyze whether the shape of the flow separation zone can be parameterized in the case of water flow over bedforms. To this end, experiments of turbulent flow over 2D subaqueous bedforms are analyzed, with different bedform heights and aspect ratios (ratio of dune height to dune length), and under various flow conditions.

In Section 2, an overview of the data used in this paper is given, and velocity profiles are analyzed to determine the shape of the flow separation zone for the different experiments. In Section 3, the separation streamline is parameterized using a third-order polynomial function, which is fitted to the individual experiments. The parameters or bedform properties controlling the dimensions of the flow separation zone are then investigated, resulting in an estimate of the length of the flow separation zone based on bedform properties. This allows imposition of the shape of the separation streamline, both at the flow separation point and at the flow reattachment point. The paper shows that the shape of the flow separation zone can be estimated independently of flow conditions, using solely bedform properties.

2. Flow Separation

2.1. Used Data Sets

The parameterization of the separation streamline requires detailed measurements of the reverse flow near the bed inside the flow separation zone, and hence only flume data are detailed enough to use for the parameterization. The data used in the present paper is summarized in Table 1, where a sub-division is made between: *i*) dunes with a horizontal bed at the flow separation point, *ii*) dunes with a negative slope at the flow separation point, and *iii*) backward-facing steps. All measurements comprise time-averaged velocity data.

In cases where bed load transport is dominant, dunes are often asymmetric with a leeside slope at the angle-of-repose ($\sim 30°$), and a region of permanent flow separation in the lee (Figure 1a) [*Smith and McLean*, 1977; *Kostaschuk and Villard*, 1996; *Best*, 2005]. Part of the data used consists of flume experiments with such dunes [*Termes*, 1984; *Van Mierlo and De Ruiter*, 1988; *Nelson et al.*, 1993; *McLean et al.*, 1999]. In nature, however, dunes are often of more complex shape. Therefore, dunes with negative slopes at the brinkpoint, the point where the leeside slope suddenly changes to the angle-of-repose (Figure 1b), are also included [*Buckles et al.*, 1984; *Kornman*, 1995; *Bennett and Best*, 1995]. Since flow separation over backward-facing steps is largely similar to that over dunes with angle-of-repose slip faces, experiments with backward-facing steps are also included in the analysis [*Raudkivi*, 1963; *Nakagawa and Nezu*, 1987; *Etheridge and Kemp*, 1978].

For the experiments with backward-facing steps, the separation point is located at the edge of the step. In the case of dunes, separation is assumed to occur at the brinkpoint, the point where the leeside slope suddenly changes to the angle-of-repose. For most experiments this point is clearly defined, except for the experiments of *Buckles et al.* [1984] and *Bennett and Best* [1995]. For these two experiments, the location of the brinkpoint is estimated at the point where the bed slope is about $-6°$, by analyzing the point where the leeside slope has the sharpest decline (exact locations can be found in Table 1).

2.2. Shape of the flow separation zone

Inside the flow separation zone, a recirculation eddy with reverse flow near the bed is present. This means that the net discharge through a vertical cross-section between the bed and the separation streamline is zero. In other words, the upstream directed discharge between the bed and the point of zero velocity is equal to the downstream directed discharge between the point of zero velocity and the separation streamline. Based on this assumption, the vertical position of the separation streamline ($z = z_{\mathrm{sep}}$) is found from:

$$\int_{z_{\mathrm{b}}}^{z_{\mathrm{sep}}} u(z)dz = 0, \quad (1)$$

where z is the vertical coordinate, with the bed at $z = z_{\mathrm{b}}$.

Figure 2 shows cubic interpolated velocity data, the points of zero velocity (i.e., $u(z) = 0$) and the separation streamline for experiment T5 of *Van Mierlo and De Ruiter* [1988] (computed z_{sep}-values are linearly connected for clarity). It should be noted that measurements over the steep leeside slope of dunes are least detailed, and that extrapolation over a significant portion of the velocity profile within the flow separation zone must be made, leading to the highest uncertainty in the location of the separation streamline (z_{sep}) in that region.

Kroy et al. [2002] parameterize the shape of the separation streamline by imposing a smooth connection at both the flow separation and reattachment point. They estimated the length of the flow separation zone (L_{s}) based on a pre-defined maximum slope of the separation streamline ($-14°$). Since *Kroy et al.* [2002] studied solitary dunes, the flow reattachment point occurs on a flat bed. In Figure 2, the parameterization of *Kroy et al.* [2002] for the shape of the separation streamline is included. For most of the experiments analyzed in the present paper, and especially when the bed is horizontal at the flow separation point (i.e. $\alpha_{\mathrm{s}} = 0$, Figure 1a), the parameterization of *Kroy et al.* [2002] turns out to fit the zero velocity data, instead of the separation streamline. This is mainly caused by the assumption of *Kroy et al.* [2002] that the length of flow separation is found from imposing a maximum slope of the separation streamline, and the assumption that the separation streamline smoothly connects to a flat bed at the reattachment point.

3. Parameterization of the Separation Streamline

In this section, a separation streamline $s(x)$ is determined for each individual experiment, by fitting a third-order polynomial function in x, the distance from the flow separation point, to the vertical locations $z = z_{\mathrm{sep}}$ found from Eq. (1). To enable comparison between the experiments, both the longitudinal coordinate x and the vertical coordinate z are scaled against the brinkpoint height of a bedform (H_{b}). Once the separation streamline is known, the reattachment point can be determined, and it is investigated which parameters control the length of the flow separation zone.

3.1. Determination of Separation Streamline

The separation streamline is parameterized using the same third-order polynomial function as used by *Kroy et al.* [2002]:

$$\tilde{s}(\xi) = \frac{s(\xi)}{H_\mathrm{b}} = s_3\,\xi^3 + s_2\,\xi^2 + s_1\,\xi + s_0, \tag{2}$$

where $\xi = (x - x_\mathrm{s})/H_\mathrm{b}$, and $s_0 \ldots s_3$ are coefficients. The shape of the separation streamline, as illustrated in Figure 2, can be approximated by imposing a smooth connection of the separation streamline to the bed at the flow separation point ($\xi = 0$), yielding for coefficients s_0 and s_1:

$$s_0 = \tilde{s}(0) = 1 \tag{3}$$

$$s_1 = \frac{d\tilde{s}(0)}{d\xi} = \tan\alpha_\mathrm{s} \tag{4}$$

Kroy et al. [2002] imposed two conditions at the flow reattachment point as well, however in our case the flow reattachment point is not known a priori. Therefore, the coefficients s_2 and s_3 are fitted to the separation streamlines as obtained in Section 3.1. The fitting-procedure results in a separation streamline for each individual experiment, and Figure 3 shows the results for four experiments of *McLean et al.* [1999].

For the experiment of *Termes* [1984] and *Kornman* [1995] it was necessary to set coefficient s_3 to zero in Eq. (2), since too few velocity profiles are located within the flow separation zone. For the experiments of *Buckles et al.* [1984] and *Nelson et al.* [1993], it was also necessary to use $s_3 = 0$, since otherwise no monotonic decreasing regression line was found, and consequently no reattachment point could be found.

To use the parameterized separation streamline in a morphodynamic model, it is important to describe the shape of the separation streamline correctly. This paper shows that the shape of the separation zone is captured with sufficient accuracy using a third-order polynomial function, with coefficients s_0 and s_1 set by realistic boundary conditions, and setting coefficients s_2 and s_3 using regression analysis. The observed behaviour that the separation streamline reattaches downstream at a certain angle (Figure 2), is also captured by the parameterization.

Table 1 lists the coefficients of determination for the fitted separation streamlines (R^2). Especially for the experiments of *McLean et al.* [1999], *Van Mierlo and De Ruiter* [1988] and experiments with backward-facing steps good fits are obtained. By using a second-order polynomial function, the overall shape of the separation zone could not be captured, especially near the region of flow reattachment. Extending the parameterization to a fourth-order polynomial function yielded unrealistic separation zone shapes, since the extra fitting coefficient led to fitting noise, rather than the average shape of the flow separation zones. *Schatz and Herrmann* [2006] used an elliptical function to parameterize the separation streamline for air flow over aeolian dunes. Their method also requires four coefficients, however to set these coefficients, the reattachment point has to be known a priori.

3.2. Determination of the Flow Reattachment Point

For each experiment, the shape of the flow separation zone is now known, allowing determination of the (time-averaged) location of the flow reattachment point. However, since the experiments used in this paper are performed with different bedform geometries (i.e. different bedform heights and/or lengths, Table 1), the bed slope at the flow reattachment point is not equal between the different experiments. To be able to compare between the various experiments, a location x_{rt} is defined, where the cubic separation streamline would intersect a flat bed whose elevation is the same as the trough elevation (Figure 1a).

This defines the separation zone length $L_{\mathrm{st}} = x_{\mathrm{rt}} - x_{\mathrm{s}}$, and a nondimensional separation zone length $L'_{\mathrm{st}} = L_{\mathrm{st}}/H_{\mathrm{b}}$. The angle of the separation streamline with the hypothetical flat bed (dash-dotted lines in the figures) is defined as $\tan\alpha_{\mathrm{rt}}$. At the reattachment point ($\xi = L'_{\mathrm{st}}$) this yields:

$$\tilde{s}(L'_{\mathrm{st}}) = 0 \tag{5}$$

$$\frac{d\tilde{s}(L'_{\mathrm{st}})}{d\xi} = \tan\alpha_{\mathrm{rt}} \tag{6}$$

Together with Eqs. (3) and (4) this yields:

$$s_3 {L'_{\mathrm{st}}}^3 + s_2 {L'_{\mathrm{st}}}^2 + \tan\alpha_{\mathrm{s}} L'_{\mathrm{st}} + 1 = 0 \tag{7}$$

and

$$3\, s_3 {L'_{\mathrm{st}}}^2 + 2\, s_2 L'_{\mathrm{st}} + \tan\alpha_{\mathrm{s}} = \tan\alpha_{\mathrm{rt}} \tag{8}$$

Using the fitted curves determined in Section 3.1, Eq. (7) is solved to obtain L'_{st}, and Eq. (8) yields $\tan\alpha_{\mathrm{rt}}$ for each individual experiment. Results are summarized in Table 1, and for experiments ML4-7 the positions of $\xi = L'_{\mathrm{st}}$ are given in 3.

3.3. Length of the Flow Separation Zone

Figure 4 shows that the length of the flow separation zone increases for increasing brinkpoint heights (Figure 4a), and that the nondimensional length of the flow separation zone ($L'_{\mathrm{st}} = L_{\mathrm{st}}/H_b$) varies roughly between 4 and 6. This range is confirmed by various sources, with the nondimensional separation zone length often reported around 4-6 [e.g., *Engel*, 1981; *Van Mierlo and De Ruiter*, 1988; *Niño et al.*, 2002; *Fernandez et al.*, 2006]. Figure 4b-d show no obvious relationship between characteristic flow parameters and the flow separation zone length. This could also be concluded from Figure 3, showing largely identical separation streamlines for four experiments where the fixed dune shape is equal, but flow conditions are different. It is also in agreement with *Engel* [1981] who showed experimentally that the nondimensional length of the flow separation zone is largely independent of the Froude number and the relative water depth (ratio of water depth to dune height), and with *Walker and Nickling* [2002], who stated that the reattachment distance behind desert dunes only slightly increased with incident wind speed.

Several authors suggest that the length of the flow separation zone is controlled, apart from brinkpoint height, by the local bed slope at the flow separation point [*Paarlberg et al.*, 2005; *Schatz and Herrmann*, 2006]. Therefore, Figure 5 shows the nondimensional length of the flow separation zone as a function of the local bed slope at the separation point. The experiments used in the present analysis have either a horizontal bed or a negative bed slope at the flow separation point (i.e. $\tan\alpha_\mathrm{s} <= 0$, Table 1). Four slope-classes are used, and each class is represented by a mean its standard deviation. Linear regression through the data yields (Figure 5):

$$L'_\mathrm{st} = 6.48 \tan\alpha_\mathrm{s} + 5.17 \tag{9}$$

By performing numerical simulations of air flow over fixed isolated aeolian dunes, *Schatz and Herrmann* [2006] also found a linear relation between the separation zone length and the bed slope at the flow separation point. *Schatz and Herrmann* [2006] found the nondimensional flow separation zone length to extend roughly 10-30% further downstream than found in this paper (Figure 5). In their conceptual model of leeside airflow however, *Walker and Nickling* [2002] suggest that the separation zone extends further over isolated solitary dunes than over closely spaced dunes because of decreased surface roughness. *Schatz and Herrmann* [2006] showed using a numerical simulation that the separation zone length over closely spaced dunes with a horizontal bed at the flow separation point (i.e. $\tan\alpha_\mathrm{s} = 0$), is about 25% smaller than over isolated dunes. This means that for dunes with a horizontal bed, *Schatz and Herrmann* [2006] found a nondimensional separation zone length of $L'_{\mathrm{st}} \approx 4.85$, which is well within the range of L'_{st} found in this paper (Figure 5).

3.4. Parameterization Based on Bedform Properties

The length of the flow separation zone is shown to be largely independent of flow conditions (Figure 4b-d), but depends on brinkpoint height (Figure 4a) and bed slope at the flow separation point (Figure 5). Therefore, the four coefficient $s_0 \ldots s_3$ are determined based on bedform properties. Coefficients s_0 and s_1 are set using Eqs. (3) and (4). The remaining coefficients s_2 and s_3 can be determined from Eqs. (7) and (8), if the location of the reattachment point and the slope of the separation streamline at the flow reattachment point are known. The position of the flow reattachment point ($\xi = L'_{\mathrm{st}}$) can be estimated using Eq. (9) with the brinkpoint height and the bed slope at the flow separation point as inputs. For the coefficients s_2 and s_3 this yields:

$$s_3 = \frac{\tan \alpha_{\mathrm{rt}}}{{L'_{\mathrm{st}}}^2} + \frac{\tan \alpha_{\mathrm{s}}}{{L'_{\mathrm{st}}}^2} + \frac{2}{{L'_{\mathrm{st}}}^3} \tag{10}$$

$$s_2 = -s_3 L'_{\mathrm{st}} - \frac{\tan \alpha_{\mathrm{s}}}{L'_{\mathrm{st}}} - \frac{1}{{L'_{\mathrm{st}}}^2} \tag{11}$$

In the case of a horizontal bed at the flow separation point (i.e. $\tan \alpha_{\mathrm{s}} = 0$), the average angle of the separation streamline at the reattachment point is $\tan \alpha_{\mathrm{rt}} = -0.53$ ($\sigma = 0.11$), yielding $s_3 = -5.4 \times 10^{-3}$ and $s_2 = -9.7 \times 10^{-3}$. In the case of a negative bed slope at the flow separation point, the angle of the separation streamline at the flow reattachment point is not known, because only limited data for these cases are available. To be able to use one boundary condition less at the flow reattachment point, the coefficient s_3 is set to zero in Eqs. (10) and (11), if $\tan \alpha_{\mathrm{s}} < 0$.

The shape of the flow separation zone can now be estimated with Eq. (2), using Eqs. (3)– (4) and (9)–(11) to set the coefficients of the polynomial. Figure 6 compares the parameterization with the separation streamlines extracted from the experiments. To assess for each experiment how well the parameterization compares to the data, the relative error E_p between the measured positions of the separation streamlines (z_sep) and the parameterized separation streamline (z_par) is determined, for each measurement point i within the flow separation zone:

$$E_{\mathrm{p},i} = \frac{z_{\mathrm{par},i} - z_{\mathrm{sep},i}}{H_\mathrm{b}}, \qquad i = 1..N_\mathrm{p} \tag{12}$$

where N_p is the number of measurements within the flow separation zone (Table 1). For each experiment, the mean (μ_p) and standard deviation (σ_p) of the errors computed with Eq. (12) are presented in Table 1. A zero mean, together with a zero standard deviation would imply a perfect fit; a positive mean implies that the parameterized separation streamline is on average above the fitted separation streamline. The average value of the mean error μ_p is 0.02 ($\sigma = 0.14$), with an average standard deviation σ_p of 0.11 ($\sigma = 0.09$), meaning that the parameterization based on dune properties captures the average shape of the flow separation zone.

Figure 6 shows that for dunes with a horizontal bed at the flow separation point, the agreement between the data and the parameterization is fairly good, especially for the experiments of *McLean et al.* [1999] and *Van Mierlo and De Ruiter* [1988]. For backward-facing steps, the size of the flow separation zone is generally underestimated by the parameterization. This might be due to the fact that backward-facing steps have a secondary corner eddy just downstream the edge of the step near the bed. For dunes, this secondary corner eddy is not present or at least less pronounced, because the angle of the lee is about –30°, instead of –90° (i.e. vertical) for backward-facing steps.

The bottom four plots in Figure 6 consider the experiments with a negative bed slope at the flow separation point, where the coefficient s_3 is set to zero. Also here, good agreement is observed between the data and the parameterization.

4. Discussion

4.1. Application of the Parameterization in a 2DV Morphodynamic Model

The aim for future research is to use the proposed parameterization in a two-dimensional vertical (2DV) dune development model where the flow is treated as hydrostatic, meaning that the details of separated flows cannot be predicted [e.g. the model described in *Paarlberg et al.*, 2005]. Following the approach of *Kroy et al.* [2002], the parameterized separation streamline can be used to provide an artificial 'bed' over which the hydrostatic assumption is approximately true. Thus only the hydrostatic flow outside the flow separation zone has to be calculated, which saves the computational effort related to modelling the flow within and around the flow separation zone.

Initial results indicate that river dune migration and formation can be captured with a morphodynamic model where the flow separation zone behaviour is parameterized [see *Paarlberg et al.*, 2006]. Using this approach, details related to the flow behaviour within the flow separation zone, such as the shear layer developing downstream of the flow separation point [e.g., *McLean et al.*, 1999; *Fernandez et al.*, 2006], are not included. For the aeolian case, *Kroy et al.* [2002] argue that dune migration and formation do not very sensitively depend on the flow behaviour within the flow separation zone. Although the process of flow separation in unidirectional air and water flows is quite similar, future research should investigate whether it is sufficient to know solely the shape of the flow separation zone in order to facilitate predicting river dune development, or if this parameterization has to be extended with details within and around (shear layer) the flow separation zone.

4.2. Application of the 2DV Parameterization to Complex River Dune Configurations

The proposed parameterization estimates the shape of the flow separation zone in the leeside of straight-crested two-dimensional vertical (2DV) dunes, with angle-of-repose slip faces. In the field however, often more complex dune configurations occur. In large rivers, the average leeside slope of dunes is often lower than about 8° [*Best*, 2005]. *Best and Kostaschuk* [2002] showed that the flow separation zone in the leeside of a low-angle dune, with a maximum leeside slope of 14°, is non-permanent with intermittent flow separation for up to 4% of the time. Additionally, river dunes often have 3D structures, such as amplitude variations or crestline curvature. *Allen* [1968] illustrated flow patterns over 3D dunes revealing complex flow separation zone dynamics due to generated vorticity and convergence and divergence of flow [*Best*, 2005]. This raises the question how to apply the proposed separation zone parameterization to low-angle dunes and 3D dune configurations.

Since low-angle dunes possess no clearly defined (or even absent) brinkpoint, and flow separation is non-permanent, the 2DV parameterization is difficult to apply to low-angle dunes. Future studies should investigate over which leeside slopes the flow separates (defining a critical bed-slope), and to what extent. If this information is available, the parameterization can be applied using a critical bed-slope as brinkpoint; in morphological calculations, the flow separation zone should be ignored for the time it is not present. It should be noted that the morphodynamic model of *Paarlberg et al.* [2006] only considers bedload transport. Possibly this assumption limits the occurrence of low-angle dunes, since their occurrence may be related to the presence of suspended sediment transport [*Best and Kostaschuk*, 2002; *Best*, 2005].

Recent studies by *Venditti* [2003] and *Maddux et al.* [2003a, b] showed that the flow field over simple regular 3D dunes is significantly different from that over their 2D counterparts. Secondary currents and flow convergence and divergence over the 3D shapes significantly influence the separation zone dynamics.

Maddux et al. [2003a, b] used fixed dunes which were 2D across the flume width, having cosine-shaped stoss-sides in streamwise direction and a variable height of the crest line, thereby creating a 3D form. Equation (9) determines the separation zone length using the bed slope at the flow separation point ($\alpha_s = 0$ in this case) and brinkpoint height as input. If the parameterization follows the main flow direction, the flow separation zone extends further downstream over the maxima in dune height, as was found by *Maddux et al.* [2003a]. However, *Maddux et al.* [2003a] also showed that secondary currents and flow convergence and divergence over the 3D shapes significantly influenced turbulence generation. This could be taken into account by including the lateral flow component, and applying the parameterization along streamlines instead of along the main flow direction.

In the experiments of *Venditti* [2003] the crest line was curved, but constant in height and cross-sectional 2D shape [see also *Best*, 2005]. For dunes where the crest-center is ahead of the banks ('lobe'-shaped dunes), the flow separation zone extended further downstream than was the case with the 2D counterpart. In situations where the crest is behind that of the banks ('saddle'-shaped dunes), convergence of flow in the hollow in the leeside suppressed the formation of a flow separation zone resulting in less turbulence but higher velocities. For these shapes our parameterization is inadequate, since the dune height is constant in these experiments. This suggests the importance of including streamlines and streamline curvature in the parameterization.

Thus to apply the separation zone parameterization to such 3D river dune configurations, the 2DV dune model should be extended to a 3D morphodynamic model, such as the model of *Hulscher* [1996]. This allows to investigate how the shape of the separation zone depends on 2DH dune-structures, e.g. by following streamlines and allowing for convergence and divergence of the parameterized separation zone. For natural irregular 3D dune fields, it might be necessary to derive a different parameterization, e.g. by including turbulent quantities or vorticity; this is beyond the scope of the present paper.

5. Conclusions

In this paper, a parameterization of flow separation associated with straight-crested subaqueous sand dunes is proposed, which can easily be applied in 2DV morphodynamic models to avoid modelling the complex flow behaviour inside the flow separation zone. The shape of the flow separation streamline can be approximated by a third-order polynomial as a function of the distance away from the flow separation point.

The length of the flow separation zone is shown to be largely independent of flow conditions, but depends on the brinkpoint height, and decreases when there is a negative bed slope at the brinkpoint. A linear relationship is found between the bed slope at the flow separation point and the length of the flow separation zone, allowing to estimate the location of the flow reattachment point. The coefficients of the third-order polynomial are set using physical boundary conditions at the flow separation point, and at the flow reattachment point. A smooth connection to the bed is assumed at the flow separation point. Since the angle of the separation streamline at the reattachment point is found to be almost constant, this angle is used as boundary condition in that point. The shape of the separation streamline, and thus the flow separation zone, is captured well by the proposed parameterization, for dunes with different heights and height to length ratios and for a wide range of flow conditions.

Acknowledgments. This work is supported by the Technology Foundation STW, the applied science division of NWO and the technology programme of the Ministry of Economic Affairs (Project No. TCB.6222). We are grateful for the data provided by Antoine Wilbers and Steve McLean, and for the suggestions of Ralph Schielen. The constructive comments of Steve McLean, Jim Best and an anonymous reviewer helped improve the manuscript significantly.

Notation

α_s	bed slope at the flow separation point, –.
α_rt	slope of the separation streamline at x_rt, –.
b	flume width, m.
E_p	relative error of the parameterization, –.
Fr	Froude number, –.
h	average flow depth, m.
H_d	bedform height (measured from crest to trough elevation), m.
H_b	brinkpoint height (measured from brinkpoint to trough elevation), m.
L_d	bedform length (measured from crest to crest), m.
L_s	length of the flow separation zone, m.
L_st	length of the flow separation zone measured from x_s to x_rt, m.
L'_st	nondimensional length of the flow separation zone ($= L_\mathrm{st}/H_b$), –.
μ_p	mean value of E_p, –.
N_p	number of points on the separation streamline to determine regression (not including the separation point), –.
N_s	number of observations in a slope-class, –.
R^2	coefficient of determination, –.
Re	Reynolds number, –.
$s(x)$	separation streamline, m.
$\tilde{s}(\xi)$	nondimensional separation streamline ($= s/H_b$), –.
$s_0 \ldots s_3$	coefficients for the separation streamline, –.
σ_p	standard deviation of E_p, –.
u	horizontal flow velocity, m s^{-1}.
U	average horizontal flow velocity, m s^{-1}.
x	horizontal streamwise coordinate, m.
x_b	x-coordinate of the brinkpoint, m.
x_r	x-coordinate of the flow reattachment point, m.
x_rt	location where the separation streamline would intersect a flat bed whose elevation is the same as the trough elevation, m.
x_s	x-coordinate of the flow separation point, m.
ξ	nondimensional distance away from the separation point ($= (x - s_s)/H_b$), –.
z	vertical coordinate, m.
z_b	bed elevation, m.
z_sep	vertical position of the fitted separation streamline, m.
z_par	vertical position of the parameterized separation streamline, m.

References

Allen, J. R. L. (1968), *Current Ripples: their relation to patterns of water and sediment motion*, 161-182 pp., North Holland Publishing Company, Amsterdam, the Netherlands.

Bennett, S. J., and J. L. Best (1995), Mean flow and turbulence structure over fixed, two-dimensional dunes: implications for sediment transport and bedform stability, *Sedimentology*, *42*(3), 491–513.

Best, J. (2005), The fluid dynamics of river dunes: A review and some future research directions, *Journal of Geophysical Research*, *110*(F04S01), doi:10.1029/2004JF000218.

Best, J., and R. Kostaschuk (2002), An experimental study of turbulent flow over a low-angle dune, *Journal of Geophysical Research*, *107*(C9, 3135), 1118–1129.

Buckles, J., T. J. Hanratty, and R. J. Adrian (1984), Turbulent flow over large-amplitude wavy surfaces, *Journal of Fluid Mechanics*, *140*, 27–44.

Engel, P. (1981), Length of flow separation over dunes, *J. Hydraul. Div. Am. Soc. Civ. Eng.*, *107*(HY10), 1133–1143.

Etheridge, D. W., and P. H. Kemp (1978), Measurements of turbulent flow downstream of a rearward-facing step, *Journal of Fluid Mechanics*, *86*(3), 545–566.

Fernandez, R., J. Best, and F. López (2006), Mean flow, turbulence structure, and bed form superimposition across the ripple-dune transition, *Water Resources Research*, *42*(W05406), doi:10.1029/2005WR004330.

Giri, S., and Y. Shimizu (2006), Numerical computation of sand dune migration with free surface flow, *Water Resources Research*, *42*(W10422), doi:10.1029/2005WR004588.

Hulscher, S. J. M. H. (1996), Tidal-induced large-scale regular bed form patterns in a three-dimensional shallow water model, *Journal of Geophysical Research*, *101*, 20,727–20,744.

Hulscher, S. J. M. H., and C. M. Dohmen-Janssen (2005), Introduction to special section on Marine Sand Wave and River Dune Dynamics, *Journal of Geophysical Research*, *110*(F04S01), doi:10.1029/2005JF000404.

Jerolmack, D. J., and D. C. Mohrig (2005), A unified model for subaqueous bed form dynamics, *Water Resources Research*, *41 (W12421)*, doi:10.1029/2005WR004329.

Julien, P. Y., G. J. Klaassen, W. B. M. Ten Brinke, and A. W. E. Wilbers (2002), Case Study: Bed resistance of Rhine River during 1998 flood, *Journal of Hydraulic Engineering*, *128*(12), 1042–1050.

Kornman, B. A. (1995), The effect of changes in the lee shape of dunes on the flow field, turbulence and hydraulic roughness, *Report on measurements R 95-1*, University of Utrecht, Utrecht, The Netherlands.

Kostaschuk, R., and P. Villard (1996), Flow and sediment transport over large subaqueous dunes: Fraser River Canada, *Sedimentology*, *43*, 849–863.

Kroy, K., G. Sauermann, and H. J. Herrmann (2002), Minimal model for aeolian sand dunes, *Physical Review E*, *66*(3).

Maddux, T. B., J. M. Nelson, and S. R. McLean (2003a), Turbulent flow over three-dimensional dunes: 1. free surface and flow response, *Journal of Geophysical Research*, *108*(F1, 6009), doi:10.1029/2003JF000017.

Maddux, T. B., J. M. Nelson, and S. R. McLean (2003b), Turbulent flow over three-dimensional dunes: 2. fluid and bed stresses, *Journal of Geophysical Research*, *108*(F1, 6010).

McLean, S. R., S. R. Wolfe, and J. M. Nelson (1999), Spatially averaged flow over a wavy boundary revisited, *Journal of Geophysical Research*, *104*(C7), 15,743–15,753.

Nakagawa, H., and I. Nezu (1987), Experimental investigation on turbulent structure of backward-facing step flow in an open channel, *Journal of Hydraulic Research*, *25*, 67–88.

Nelson, J. M., S. R. McLean, and S. R. Wolfe (1993), Mean flow and turbulence fields over 2-dimensional bed forms, *Water Resources Research*, *29*(12), 3935–3953.

Nelson, J. M., R. L. Schreve, S. R. McLean, and T. Drake (1995), Role of near-bed turbulence structure in bedload transport and bedform mechanics, *Water Resources Res.*, *31*(8), 2071–2086.

Nelson, J. M., A. R. Burman, Y. Shimizu, S. R. McLean, R. L. Shreve, and M. Schmeeckle (2005), Computing flow and sediment transport over bedforms, in *Proceedings of the 4th IAHR Symposium on River, Coastal and Estuarine Morphodynamics, Urbana, Illinois, USA*, vol. 2, edited by G. Parker and M. H. Garcia, pp. 861–872, Taylor & Francis Group, London.

Niño, Y., A. Atala, M. Barahona, and D. Aracena (2002), Discrete particle model for analyzing bedform development, *Journal of Hydraulic Engineering*, *128*(4), 381–389.

Ogink, H. J. M. (1989), Hydraulic roughness of single and compound bed forms. Part XI report on model investigations., *TOW Rivieren M 1314-XI/Q786*, Delft Hydraulics Laboratory, Delft, The Netherlands.

Onda, S., and T. Hosoda (2004), Numerical simulatin on development process of dunes and flow resistance, in *Proceedings of River Flow 2004, Napoli, Italy*, vol. 1, edited by M. Greco, A. Carravetta, and R. Della Morte, pp. 245–252, Frederico II University of Napoli, Balkema publishers, Leiden, the Netherlands.

Paarlberg, A. J., C. M. Dohmen-Janssen, S. J. M. H. Hulscher, and A. P. P. Termes (2005), A parameterization of flow separation in a river dune development model, in *Proceedings of the 4th River, Coastal and Estuarine Morphodynamics conference, Urbana, Illinois, USA*, vol. 2, edited by G. Parker and M. H. Garcia, pp. 883–895, Taylor & Francis Group, London.

Paarlberg, A. J., C. M. Dohmen-Janssen, S. J. M. H. Hulscher, J. Van den Berg, and A. P. P. Termes (2006), Modelling morphodynamic evolution of river dunes, in *Proceedings of the River flow 2006 conference, Lisbon, Portugal*, edited by Ferreira, Alves, Leal, and Corsado, pp. 969–978, Taylor & Francis Group, London.

Raudkivi, A. J. (1963), Study of sediment ripple formation, *Journal of the Hydraulics Division*, *89*(6), 15–33.

Schatz, V., and H. J. Herrmann (2006), Flow separation in the lee side of transverse dunes: A numerical investigation, *Geomorphology*, *81*, 207–216, doi:

10.1016/j.geomorph.2006.04.009.

Smith, J. D., and S. R. McLean (1977), Spatially-averaged flow over a wavy surface, *Journal of Geophysical Research*, *82*, 1735–1746.

Sumer, B. M., L. H. C. Chua, N. S. Cheng, and J. Fredsøe (2003), Influence of turbulence on bed load sediment transport, *Journal of Hydraulic Engineering*, *129*(8), 585–596.

Termes, A. P. P. (1984), Water movement over a horizontal bed and solitary sand dune, *Rep. No. R/1984/H/8*, Delft Univ. Tech., Delft, The Netherlands.

Tjerry, S., and J. Fredsøe (2005), Calculation of dune morphology, *Journal of Geophysical Research*, *110*(F04013), doi:10.1029/2004JF000171.

Van den Berg, J., and R. Van Damme (2005), Sand wave simulation on large domains, in *Proceedings of the 4th conference on River, Coastal and Estuarine Morphodynamics, Urbana, Illinois, USA*, vol. 2, edited by G. Parker and M. H. Garcia, pp. 991–997, Taylor & Francis Group, London.

Van Mierlo, M. C. L. M., and J. C. C. De Ruiter (1988), Turbulence measurements above artificial dunes; Report on measurements, *Report Q789*, WL | Delft Hydraulics, Delft, The Netherlands.

Vanoni, V. A., and L. S. Hwang (1967), Relation between bed forms and friction in streams, *Journal of the Hydraulic Division*, *93*, 121–144.

Venditti, J. G. (2003), Initiation and development of sand dunes in river channels, Ph.D. thesis, University of Britisch Columbia.

Walker, I. J., and W. G. Nickling (2002), Dynamics of secondary airflow and sediment transport over and in the lee of transverse dunes, *Progress in Physical Geography*, *26*(1), 47–75, doi:10.1191/0309133302pp325ra.

Wijbenga, J. H. A. (1990), Flow resistance and bedform dimensions for varying flow conditions; a literature review (main text and annexes), *TOW Rivers Report Q785*, WL | Delft Hydraulics, Delft, The Netherlands.

Figure 1. Schematic representation of flow separation in the lee of a dune with: a) horizontal bed at the flow separation point, and b) negative bed slope at the flow separation point, including a sketch of the separation streamline. Flow separation is assumed to occur at the brinkpoint (x_b). See Notation section for used parameters.

Figure 2. Illustration of velocity data, zero velocity points and separation streamline for experiment T5 of *Van Mierlo and De Ruiter* [1988]. The separation streamline is compared to the parameterization of *Kroy et al.* [2002].

Figure 3. Separation streamlines for data of *McLean et al.* [1999]. Dashed lines are the regressed separation streamlines (symbols at trough elevation distinguish the four experiments).

Figure 4. (a) Relationship between the brinkpoint height and the (dimensional) separation zone length (see Figure 1 and Notation section for parameters, and Table 1 for abbreviations used in the legend). The data for the experiment of *Raudkivi* [1963] is scaled by a factor 1/6 for clarity with actual numbers given in the figure. The dotted lines represent $L_{\mathrm{st}} = 4H_{\mathrm{b}}$ and $L_{\mathrm{st}} = 6H_{\mathrm{b}}$. (b-d) Dependency of the nondimensional separation zone length on the following flow parameters: (b) ratio of water depth to brinkpoint height, (c) Froude number, and (d) Reynolds number.

Figure 5. Nondimensional length of the flow separation zone (L'_{st}) as a function of the bed slope at the separation point ($\tan \alpha_{\mathrm{s}}$). The data are grouped into four slope-classes with N_s the number of observations in that class; per class the mean and standard deviation are shown. The solid line is a linear fit trough the mean nondimensional separation zone lengths, and the dash-dotted line is Equation (2) in *Schatz and Herrmann* [2006].

Figure 6. Comparison of the parameterization with the separation streamlines found from the regression analysis. Bed profiles are underlain by a gray shading for clarity. Within the flow separation zone, the solid lines represent the parameterization, and the symbols represent the measured vertical positions along the separation streamlines (z_{sep}) with the dotted lines the fits through these positions.

Table 1. Flow conditions, bedform specifications and results of data analysis for the experiments used in this paper.

Authors	I. Flow conditions					II. Bedform specifications				III. Parameterization					
	b [m]	h [m]	U [m s^{-1}]	Fr [-]	Re (10^5)	H_d [m]	H_b [m]	L_d [m]	$\tan\alpha_\mathrm{s}$ [-]	N_p [-]	R^2 [-]	L'_st [-]	$\tan\alpha_\mathrm{rt}$ [-]	μ_p [-]	σ_p [-]
ML2	0.90	0.16	0.39	0.31	0.62	0.04	0.04	0.81	0.00	8	0.97	4.79	–0.52	0.092	0.082
ML3	0.90	0.55	0.28	0.12	1.53	0.04	0.04	0.81	0.00	7	0.99	4.69	–0.57	0.072	0.087
ML4	0.90	0.16	0.38	0.30	0.60	0.04	0.04	0.41	0.00	7	0.99	4.65	–0.62	0.064	0.066
ML5	0.90	0.16	0.20	0.16	0.32	0.04	0.04	0.41	0.00	8	1.00	5.04	–0.52	0.034	0.020
ML6	0.90	0.30	0.54	0.31	1.62	0.04	0.04	0.41	0.00	7	1.00	4.45	–0.59	0.116	0.094
ML7	0.90	0.56	0.24	0.10	1.34	0.04	0.04	0.41	0.00	7	0.96	4.55	–0.67	0.056	0.103
MR5	1.50	0.25	0.44	0.28	1.11	0.08	0.08	1.60	0.00	6	0.99	5.43	–0.61	–0.081	0.081
MR6	1.50	0.33	0.55	0.30	1.84	0.08	0.08	1.60	0.00	4	0.99	5.29	–0.51	–0.008	0.039
Te1	0.50	0.23	0.50	0.33	1.16	0.06	0.06	0.50	0.00	2	1.00	3.86	–0.52	0.211	0.435
Te2	0.50	0.23	0.50	0.33	1.16	0.06	0.06	0.50	0.00	2	1.00	4.75	–0.42	0.114	n/a
Ne1	0.70	0.20	0.51	0.37	0.99	0.04	0.04	0.80	0.00	4	0.86	3.90	–0.51	0.310	0.150
Ko3a	1.50	0.68	0.59	0.23	4.00	0.15	0.15	3.75	0.00	2	n/a	5.03	–0.40	0.084	0.062
Ko3b	1.50	0.66	0.81	0.32	5.33	0.15	0.15	3.75	0.00	2	n/a	5.04	–0.40	0.092	0.048
Ko2a	1.50	0.68	0.66	0.26	4.53	0.15	0.13	3.75	–0.08	3	0.92	5.01	–0.24	–0.036	0.126
Ko2b	1.50	0.67	0.66	0.26	4.41	0.15	0.13	3.75	–0.08	3	0.96	5.17	–0.23	–0.139	0.092
Ko1a	1.50	0.68	0.67	0.26	4.56	0.15	0.10	3.75	–0.16	2	n/a	3.88	–0.20	0.076	0.019
Ko1b	1.50	0.67	0.66	0.26	4.45	0.15	0.10	3.75	–0.16	2	n/a	4.11	–0.17	0.046	0.061
BB1	0.30	0.10	0.57	0.58	0.57	0.05	0.04[a]	0.67	–0.10	10	0.76	4.47	–0.51	–0.105	0.092
Bu1	0.61	0.05	0.51	0.75	0.24	0.01	0.01[b]	0.05	–0.10	5	0.65	4.38	–0.26	0.073	0.104
NN1	0.30	0.06	0.14	0.19	0.08	0.02	0.02	n/a	0.00	5	0.99	6.69	–0.43	–0.336	0.295
NN3	0.30	0.11	0.22	0.22	0.23	0.02	0.02	n/a	0.00	5	0.98	5.78	–0.36	–0.012	0.102
Ra1	0.50	1.19	1.31	0.38	15.54	0.91	0.91	n/a	0.00	7	0.98	5.80	–0.76	–0.235	0.132
EK1	0.15	0.20	0.26	0.19	0.52	0.01	0.01	n/a	0.00	4	1.00	5.06	–0.64	–0.040	0.013

Authors: ML: *McLean et al.* [1999]; MR: *Van Mierlo and De Ruiter* [1988]; Te: *Termes* [1984]; Ne: *Nelson et al.* [1993]; Ko: *Kornman* [1995]; BB: *Bennett and Best* [1995]; Bu: *Buckles et al.* [1984]; NN: *Nakagawa and Nezu* [1987]; Ra: *Raudkivi* [1963]; EK: *Etheridge and Kemp* [1978]; used numbers refer to numbering used by authors. See Notation section for used parameters. [a]: brinkpoint assumed at $x = 0.05$ m, $z = 0.041$ m in author's data; [b]: brinkpoint assumed at $x = 0.0025$ m, $z = 0.01$ m in author's data.

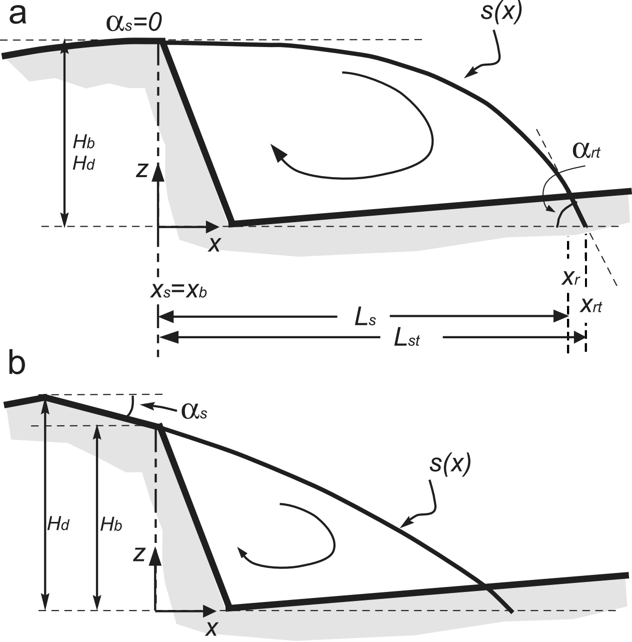
a
$\alpha_s=0$
$s(x)$
H_b
H_d
z
x
α_{rt}
$x_s=x_b$
x_r
x_{rt}
L_s
L_{st}
b
α_s
$s(x)$
H_d
H_b
z
x

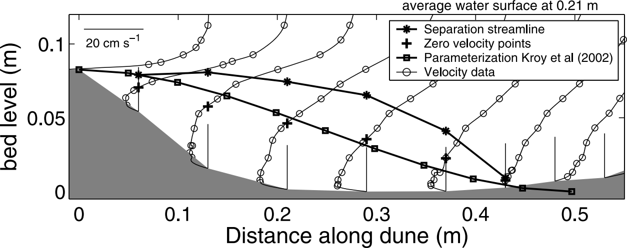
average water surface at 0.21 m
20 cm s^{-1}
Separation streamline
Zero velocity points
Parameterization Kroy et al (2002)
Velocity data
bed level (m)
0.1
0.05
0
0
0.1
0.2
0.3
0.4
0.5
Distance along dune (m)

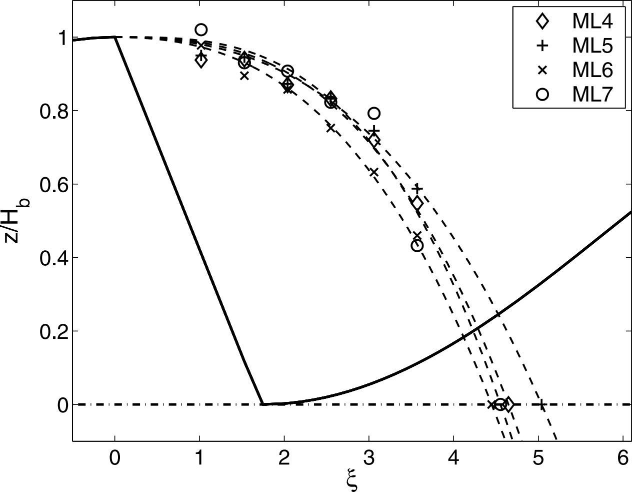
ML4
ML5
ML6
ML7
z/H_b
ξ
1
0.8
0.6
0.4
0.2
0
0
1
2
3
4
5
6

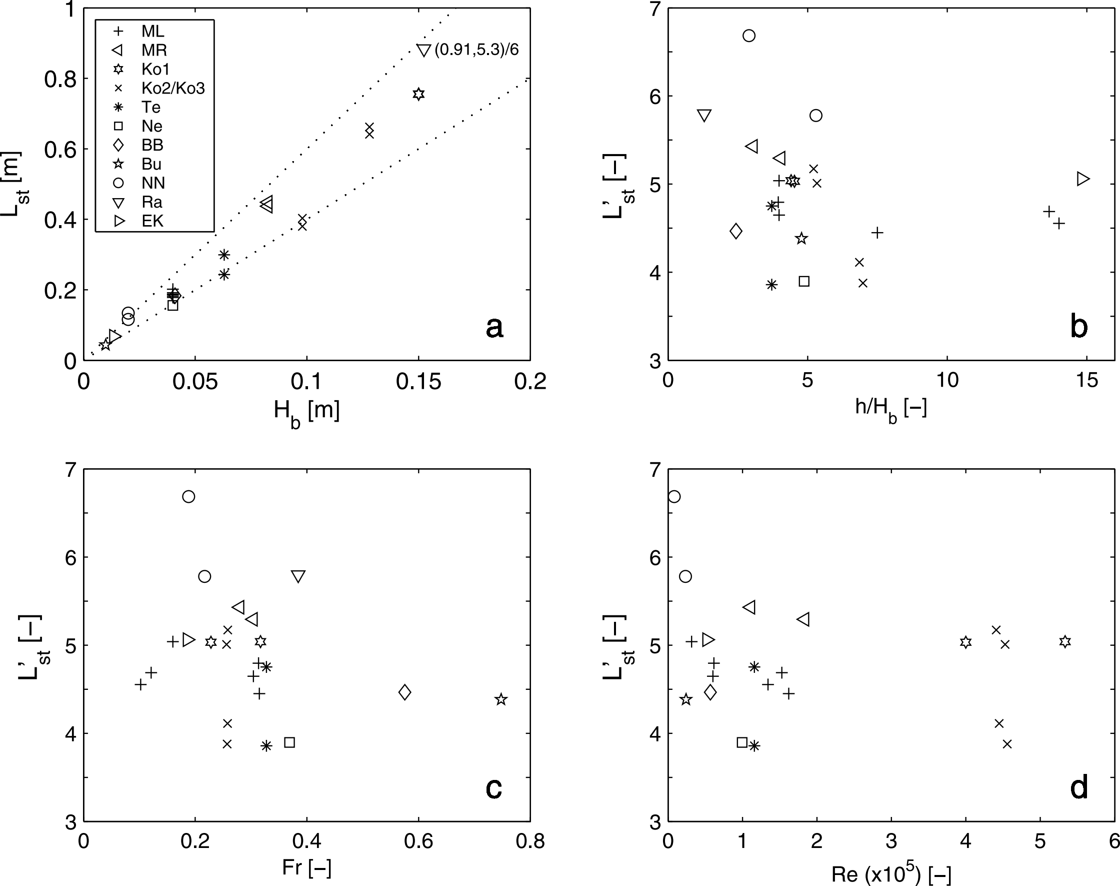
ML
MR
Ko1
Ko2/Ko3
Te
Ne
BB
Bu
NN
Ra
EK
(0.91,5.3)/6
a
b
c
d
L_{st} [m]
H_b [m]
L'_{st} [–]
h/H_b [–]
Fr [–]
Re (x10^5) [–]

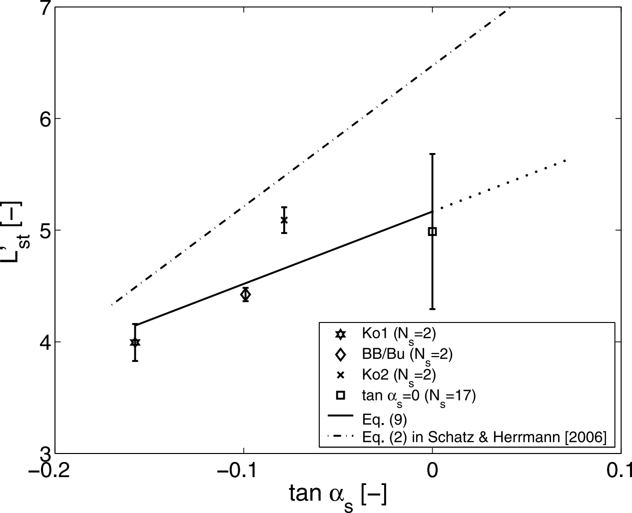

7
6
5
4
3
L'st [–]
−0.2
−0.1
0
0.1
tan αs [–]
Ko1 (Ns=2)
BB/Bu (Ns=2)
Ko2 (Ns=2)
tan αs=0 (Ns=17)
Eq. (9)
Eq. (2) in Schatz & Herrmann [2006]

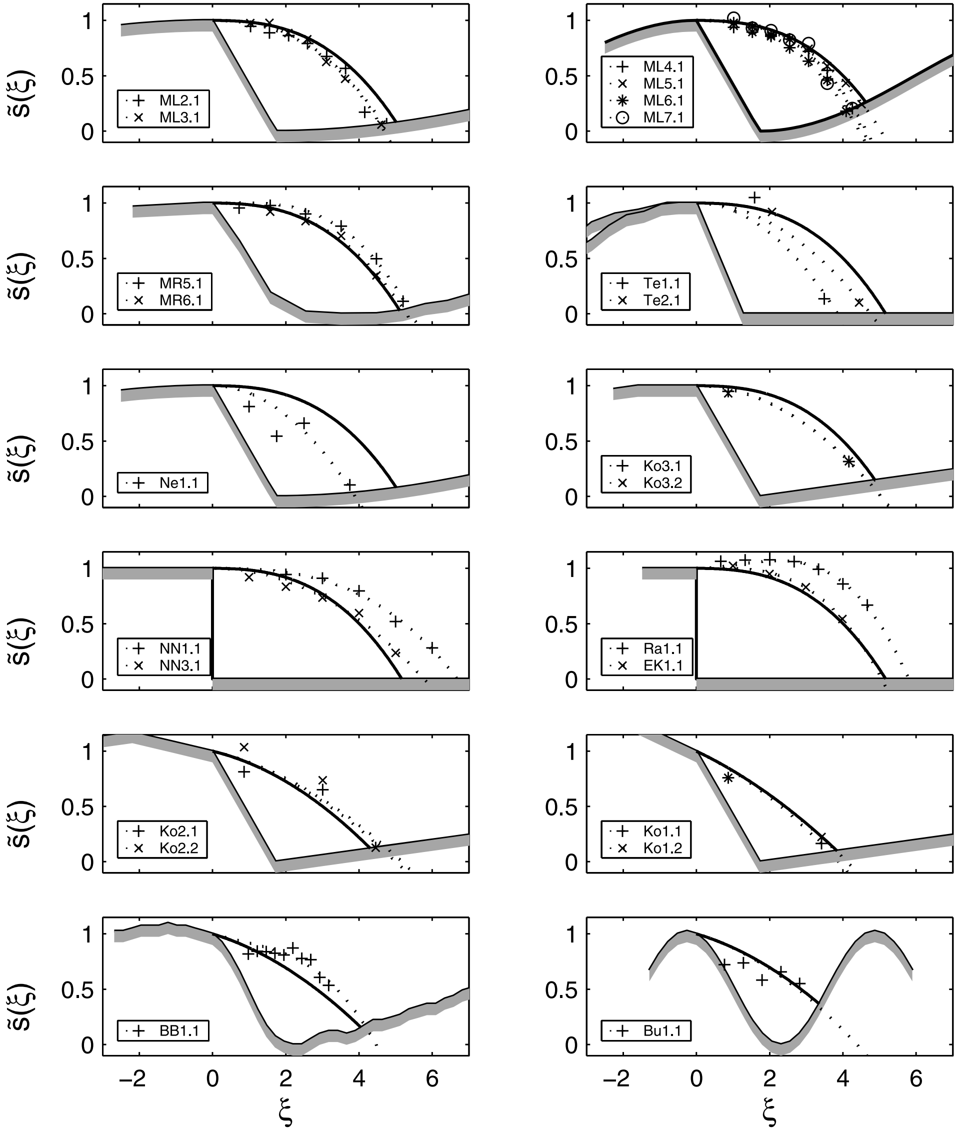

ML2.1
ML3.1
ML4.1
ML5.1
ML6.1
ML7.1
MR5.1
MR6.1
Te1.1
Te2.1
Ne1.1
Ko3.1
Ko3.2
NN1.1
NN3.1
Ra1.1
EK1.1
Ko2.1
Ko2.2
Ko1.1
Ko1.2
BB1.1
Bu1.1
$\tilde{s}(\xi)$
ξ